



## Full length article

## Underappreciated roles of soil nitrogen oxide emissions on global acute health burden

Song Liu<sup>a</sup>, Jing Wei<sup>b</sup>, Xicheng Li<sup>a</sup>, Lei Shu<sup>c</sup>, Jiaming Zhang<sup>a</sup>, Tzung-May Fu<sup>a,d,e</sup>, Xin Yang<sup>a,d,e</sup>, Lei Zhu<sup>a,d,e,\*</sup>

<sup>a</sup> School of Environmental Science and Engineering, Southern University of Science and Technology, Shenzhen 518055, China

<sup>b</sup> Department of Atmospheric and Oceanic Science, Earth System Science Interdisciplinary Center, University of Maryland, College Park, MD, USA

<sup>c</sup> School of Geographical Sciences, Fujian Normal University, Fuzhou 350117, China

<sup>d</sup> Guangdong Provincial Observation and Research Station for Coastal Atmosphere and Climate of the Greater Bay Area, Shenzhen 518055, China

<sup>e</sup> Shenzhen Key Laboratory of Precision Measurement and Early Warning Technology for Urban Environmental Health Risks, School of Environmental Science and Engineering, Southern University of Science and Technology, Shenzhen 518055, China

## ARTICLE INFO

Handling Editor: Xavier Querol

**Keywords:**

Air pollution  
Health burden  
Soil NO<sub>x</sub>  
Machine learning  
Model simulation

## ABSTRACT

The recognized importance of ambient fine particulate matter (PM<sub>2.5</sub>), ozone (O<sub>3</sub>), and nitrogen dioxide (NO<sub>2</sub>) on human health has prompted the world to enact increasingly strict regulations on anthropogenic nitrogen oxides (NO<sub>x</sub>) emissions. However, the health concerns from soil NO<sub>x</sub>, potentially driven by fertilizer input but conventionally categorized as natural sources, remain less studied. Here, we emphasize the underappreciated roles of soil NO<sub>x</sub> emissions on health burden attributable to short-term PM<sub>2.5</sub>, O<sub>3</sub>, and NO<sub>2</sub> exposure. Globally, we quantify acute health effects using machine-learning-based daily exposure estimates and identify influences of soil NO<sub>x</sub> emissions based on chemical transport model simulations. We find that 72.3% of the globe is affected by soil NO<sub>x</sub> emissions, whose contributions to short-term PM<sub>2.5</sub>, O<sub>3</sub>, and NO<sub>2</sub> pollution lead to 13.9 (95% Confidence Interval [CI]: 9.1–18.8), 26.0 (18.2–34.2), and 13.9 (10.3–17.5) thousand premature mortality, respectively, in 2019. With distinct variations in regions, seasons, and pollutants, soil NO<sub>x</sub>-originated air pollution poses a global health concern, particularly for developing regions and intensively agricultural areas. In response to the intensive fertilizer use, South Asia, Southern Sub-Saharan Africa, and Central Europe witness the largest soil NO<sub>x</sub>-related health burden of up to 1.6 (95% CI: 1.1–2.1) mortality per 100k population. The overall health risk peaks in May, with O<sub>3</sub> pollution typically dominating the soil NO<sub>x</sub>-attributable health burden during warm seasons and NO<sub>2</sub> or PM<sub>2.5</sub> during cold months. Our study highlights the necessity of dynamically adapted agricultural strategies for health-oriented multi-pollutant control, among which the improved use of synthetic fertilizers deserves priority under the ever-changing climate.

## 1. Introduction

Air pollution has a widely recognized impact on human health. The latest Global Burden of Disease (GBD) 2021 study ([GBD 2021 Risk Factors Collaborators, 2024](#)) identifies fine particulate matter (PM<sub>2.5</sub>) pollution as the leading contributor to the global disease burden. The emerging importance of ozone (O<sub>3</sub>) and the introduction of nitrogen dioxide (NO<sub>2</sub>) as a new risk factor add extra dimensions to the air pollution picture. Emissions of nitrogen oxides (NO<sub>x</sub>≡ NO+NO<sub>2</sub>), the shared precursors of PM<sub>2.5</sub> and O<sub>3</sub>, originate from both anthropogenic sources (e.g., fuel combustion from power plants, industrial processes, and transportation) and natural sources (e.g., soil) ([Hudman et al., 2012; Seinfeld and Pandis, 2016; Hoesly et al., 2018](#)). Despite the influences from natural nitrogen pool as well as agricultural fertilizer input,

soil NO<sub>x</sub> emissions are conventionally not considered in the current control measures and health management ([Zhang et al., 2019](#)). In the study, we quantify the underappreciated roles of soil NO<sub>x</sub> emissions on health concerns by coupling exposure estimates, sensitivity simulations, and exposure-response functions.

Soil NO<sub>x</sub> emissions, accounting for ~15% of global NO<sub>x</sub> emissions ([Weng et al., 2020](#)), is primarily produced by microbial processes in natural and agricultural ecosystems. These emissions are dynamically controlled by diverse factors, such as soil temperature, water content, and inorganic nitrogen availability, and can be significantly altered by agricultural practices. For example, fertilization contributes up to 58% of July soil NO<sub>x</sub> emissions in North China Plain ([Lu et al., 2021](#)). While there have been limited long-term variations over the

\* Corresponding author at: School of Environmental Science and Engineering, Southern University of Science and Technology, Shenzhen 518055, China.  
E-mail address: zhul3@sustech.edu.cn (L. Zhu).

recent decades, excessive inputs of nitrogen fertilizer pose adverse impacts on air pollution and chronic health burden (Lelieveld et al., 2015), which are typically categorized as biogenic sources. Source attribution studies focusing on agricultural areas have observed soil NO<sub>x</sub>-driven increase in O<sub>3</sub> concentrations (up to 41.8%) (Sha et al., 2021; Shen et al., 2023) and extension in O<sub>3</sub> exceedance days (up to 43.5%) (Huang et al., 2023) during warm seasons.

In addition to long-term effects, short-term pollution exposure and associated acute health impacts are drawing increasing attention from the public and policy-makers. However, comprehensive assessments have been limited by the availability of high-quality air pollution data on a global and daily basis. Researchers have commonly used ground-based measurements, satellite retrievals, or chemical transport model simulations to evaluate PM<sub>2.5</sub> and O<sub>3</sub> health outcomes (Wang et al., 2020, 2021c; McDuffie et al., 2021; Li et al., 2023a). The state-of-the-art extraction and integration of these multiple information using artificial intelligence models offers an attractive option to assess exposure risk and health burden, with unique advantages of high accuracy, fine resolution, and full coverage (Xiao et al., 2021; Wei et al., 2022b,a, 2023b,a).

In this study, we apply daily full-coverage machine learning estimates for PM<sub>2.5</sub>, O<sub>3</sub>, and NO<sub>2</sub> surface concentrations in 2019 and short-term exposure-response functions to investigate premature mortality. Additionally, we isolate the contribution of soil NO<sub>x</sub> to health burden using the GEOS-Chem chemical transport model. Insights from such a global perspective are crucial for developing agriculture-relevant policies with significant health benefits, which becomes increasingly important as control of anthropogenic sources strengthens and climate warming intensifies.

## 2. Data and methods

The soil NO<sub>x</sub>-related health burden is derived by integrating daily exposure estimates, short-term exposure health risks, and modeled fractional impacts. Figure S1 illustrates the overall workflow of the method.

### 2.1. Daily air pollution exposure

We derive short-term air pollution exposure as 24-h average PM<sub>2.5</sub> concentrations, daily maximum 8-h average (MDA8) O<sub>3</sub> concentrations, and 24-h average NO<sub>2</sub> concentrations (Wei et al., 2022b,a, 2023a). These gapless pollutant data are estimated at a 10 × 10 km<sup>2</sup> resolution with artificial intelligence technique combining ground-based in situ observations, satellite remote sensing products, reanalysis data, emission inventories, and surface- and population-related datasets. See Tables S1-S3 for details of data sources.

Based on the multi-source data, we adopt a tree-based ensemble-learning extremely randomized trees (extra-trees) algorithm (Geurts et al., 2006) for modeling air pollutants, with unique advantages including stronger randomness and an anti-interference ability (Wei et al., 2021). Specifically, a 4-dimensional space-time extra-trees (4D-STET) model is developed by introducing Euclidean spherical space and triangular spiral time to better describe both the autocorrelations and differences of individual points in spatial locations and temporal series. The 4D-STET framework first use assimilation data to fill satellite gaps, e.g., caused by cloudy contaminations, and estimate surface concentrations based on input data.

The performance of daily exposure estimates is evaluated with sample-based ten-fold cross-validation in this work (Figure S2) and our previous study focusing on anthropogenic contributions to the health burden of PM<sub>2.5</sub> and O<sub>3</sub> (Liu et al., 2024). The calculated surface concentrations are generally in line with ground-based in situ observations with validated coefficients of determination of 0.93, 0.89, and 0.84, root-mean-square errors of 8.3, 9.1, and 7.5 µg m<sup>-3</sup>, and mean absolute errors of 3.9, 5.8, and 5.1 µg m<sup>-3</sup> for PM<sub>2.5</sub>, O<sub>3</sub>, and NO<sub>2</sub>, respectively.

### 2.2. Health burden due to short-term pollution exposure

We assess the premature mortality attributed to single-day pollution exposure ( $M$ ) with the human health impact function (Lelieveld et al., 2013; Dedoussi et al., 2020) as:

$$M = \frac{y_0}{365} \sum_i Pop_i [1 - RR(\Omega_i)^{-1}]. \quad (1)$$

On a GBD regional level,  $y_0$  represents the annual baseline of mortality rate in 2019 (<https://vizhub.healthdata.org/gbd-results>).  $RR(\Omega_i)$  is a log-linear concentration-response curve (Anenberg et al., 2010) indicating the relative risk subject to the exposure level  $\Omega$  in  $i$  grid. The single-day mortality is added up into monthly, seasonally, or annual sums. We apply  $RR$  for all-cause mortality as 1.0065 (95% Confidence Interval [CI]: 1.0044–1.0086) for PM<sub>2.5</sub>, 1.0043 (1.0034–1.0052) for O<sub>3</sub>, and 1.0072 (1.0059–1.0085) for NO<sub>2</sub> with an increase in pollutant concentration per 10 µg m<sup>-3</sup> following a meta-analysis study focusing on short-term exposure (Orellano et al., 2020). Theoretical minimum-risk concentrations range between 2.4 and 5.9 µg m<sup>-3</sup> for NO<sub>2</sub>, 29.1 and 35.7 ppb for O<sub>3</sub>, and 4.6 and 6.2 ppb for NO<sub>2</sub> according to the GBD 2021 study (GBD 2021 Risk Factors Collaborators, 2024). The population ( $Pop$ ) is from Gridded Population of the World (GPW) v4 (<http://sedac.ciesin.columbia.edu/data/collection/gpw-v4>).

We propagate the uncertainty in the input to the mortality estimates with the Monte Carlo simulations (Giani et al., 2020; Xiao et al., 2021). The base mortality rates and exposure-response functions with 95% CI are simulated using normal distributions. The uncertainties of the theoretical minimum-risk concentrations are simulated by uniform distribution according to the reported ranges. The uncertainties of the exposure estimates are modeled with normal distributions using the standard errors from the cross-validation assessments (i.e., 0.024, 0.013, and 0.017 µg m<sup>-3</sup> for PM<sub>2.5</sub>, O<sub>3</sub>, and NO<sub>2</sub>, respectively). We conduct 2000 independent Monte Carlo simulations by sampling from the above distributions and calculate the mortality values based on Eq. (1). The central estimate is therefore the mean of the 2000 mortality estimates, and the 95% CI is calculated from the empirical distribution. Compared to the traditional 95% CI computed only with uncertainties of the concentration-response functions, our total health burden is wider of 40.9, 92.9, and 41.3 thousand mortality for PM<sub>2.5</sub>, O<sub>3</sub>, and NO<sub>2</sub>, respectively (Figure S3).

### 2.3. Global air quality modeling

The fractional sector impacts from soil and anthropogenic NO<sub>x</sub> emissions are derived from perturbation simulations using the GEOS-Chem chemical transport model (<http://www.geos-chem.org>). The model is equipped with detailed O<sub>3</sub>-NO<sub>x</sub>-VOC-halogen-aerosol chemistry (version 12.9.3) and driven by assimilated meteorological data from the Modern-Era Retrospective Analysis for Research and Applications, Version 2 (MERRA2) (Gelaro et al., 2017). The global simulations are configured at a resolution of 2° × 2.5° with a spin-up time of 1 year. Emissions are computed with the Harmonized Emissions Component (HEMCO) (Keller et al., 2014). Anthropogenic emissions for 2019 are from the Community Emissions Data System (CEDS) inventory (Hoesly et al., 2018), covering sectors of transportation, energy, ships, residential, industrial, solvents, and waste. Biogenic emissions are calculated online using the Model of Emissions of Gases and Aerosols from Nature (MEGAN) version 2.1 (Guenther et al., 2012). Biomass burning emissions are from the fourth-generation Global Fire Emissions Database (GFED4) (Giglio et al., 2013).

Soil NO<sub>x</sub> emissions in GEOS-Chem are estimated using the Berkeley Dalhousie Soil NO<sub>x</sub> Parameterization (BDSNP) scheme (Hudman et al., 2012). This scheme considers available soil nitrogen content (from the natural pool, fertilizer application, and nitrogen deposition), soil temperature and moisture dependences, and pulsed soil emissions from wetting of dry soils. Fertilizer applications are obtained from a spatially

explicit synthetic fertilizer and manure application inventory based on year 2000 conditions (Potter et al., 2010). According to a newly public dataset (Adalibieke et al., 2023), we show in Figure S4 that the synthetic fertilizer and manure use in the base year of 2000 is similar to that in 2019 for major consumers, such as East Asia (30.0 compared with 33.6 Tg N) and High Income North America (16.8 compared with 19.0 Tg N). However, our simulations may locally underestimate soil NO<sub>x</sub> emissions due to lower fertilizer application in 2000 for India (by -29.6%) and smaller consumers (by up to -38.3%), such as Tropical Latin America and Eastern Europe.

GEOS-Chem simulations with similar configurations effectively capture patterns for air pollutants, with biases generally less than 50% when evaluated against extensive space-, aircraft-, and ground-based observations (Boersma et al., 2009; Zhu et al., 2016; David et al., 2019; Liu et al., 2023). Figure S5 and Liu et al. (2024) demonstrate that our GEOS-Chem simulations align with in situ observations, showing correlation coefficients of 0.75, 0.77, and 0.59 and relative mean biases of 30.4, 38.7, and -18.6% for PM<sub>2.5</sub>, O<sub>3</sub>, and NO<sub>2</sub>, respectively. These biases are potentially related to the uncertainties in anthropogenic and natural emissions, as well as representations of meteorological fields or chemical processes (Fritz et al., 2022). In terms of soil NO<sub>x</sub> emissions, the widely used BDSNP produces comparable results with regional top-down constraints (Huber et al., 2020) and field measurements (Lu et al., 2021) but with room for improvements in representing emission coefficient (Sha et al., 2021), temperature (Wang et al., 2021b), and moisture (Huber et al., 2023).

#### 2.4. Fractional sector impacts

Based on the zeroing-out method, we calculate the fractional impacts (*Frac*) as the relative differences between a base simulation (with standard anthropogenic and natural NO<sub>x</sub> emissions) and sensitivity simulations (with individual source sectors excluded):

$$Frac = \frac{C_{base} - C_{sensitivity}}{C_{base}}, \quad (2)$$

where *C* indicates the modeled PM<sub>2.5</sub>, O<sub>3</sub>, or NO<sub>2</sub> concentration. On top of those fractional impacts, population-weighted fractional source impacts (*F<sub>source</sub>*) are quantified as:

$$F_{source} = \frac{\sum_i Frac_i \times \Omega_i \times Pop_i}{\sum_i Pop_i} / \frac{\sum_i \Omega_i \times Pop_i}{\sum_i Pop_i}, \quad (3)$$

with  $\Omega_i$  indicating the machine-learning-derived PM<sub>2.5</sub>, O<sub>3</sub>, or NO<sub>2</sub> concentration in *i* grid. The calculated fractional source impacts (*F<sub>source</sub>*) are applied to the health burden (*M*) in Eq. (1) to quantify source impacts from soil and anthropogenic NO<sub>x</sub> emissions.

### 3. Results and discussion

#### 3.1. Soil NO<sub>x</sub> contributions to acute health burden

The estimated global soil NO<sub>x</sub> emissions are 14.5 Tg N in 2019 (Figure S6), comparable to previous bottom-up and top-down studies in the range of 6.2–16.8 Tg N (Stavrakou et al., 2008; Vinken et al., 2014; Heald and Geddes, 2016; Miyazaki et al., 2017; Weng et al., 2020). Globally, 72.3% of the continent is affected by soil NO<sub>x</sub> emissions, with at least one month of soil NO<sub>x</sub> contributions to NO<sub>2</sub> concentrations higher than 30% following Vinken et al. (2014). This impact is particularly pronounced in regions with intensive agricultural activities, such as the Indo-Gangetic Plain and North China Plain (Fig. 1a, c, e). In soil NO<sub>x</sub>-affected regions, 89.4, 81.8, and 4.4% of the area experience with pollution day(s) exceeding the World Health Organization (WHO) daily guidelines for PM<sub>2.5</sub>, O<sub>3</sub>, and NO<sub>2</sub> (15, 100, and 25 µg m<sup>-3</sup>), respectively (Figure S7). When using the WHO theoretical minimum-risk concentrations without adverse health outcomes as references (see Section 2.2), these percentages increase to 100.0, 90.8 and 33.5%.

In Fig. 1a, c, e, elevated concentrations of PM<sub>2.5</sub> (up to 105.6 µg m<sup>-3</sup> annually and 631.3 µg m<sup>-3</sup> daily) are primarily attributed to intense regional or local sources, such as biomass burning, mineral dust, fuel combustion, along with fertilizer application (McDuffie et al., 2021). In comparison, NO<sub>2</sub> levels are more sensitive to local emissions and less prone to long-range transport owing to its short atmospheric lifetime (hours near the surface), resulting in high concentrations (up to 64.5 µg m<sup>-3</sup> annually and 159.0 µg m<sup>-3</sup> daily), particularly over populated area. On the contrary, O<sub>3</sub> pollution (up to 141.4 µg m<sup>-3</sup> annually and 410.1 µg m<sup>-3</sup> daily) exhibits more complex and widespread influences, due to its non-linear responses to meteorological conditions and precursor emissions (Lyu et al., 2023). Overall, for polluted places affected by soil NO<sub>x</sub> emissions, the population-weighted average numbers of pollution days exceeding WHO daily guidelines stand at 134, 73, and 17 days, for PM<sub>2.5</sub>, O<sub>3</sub>, and NO<sub>2</sub>, respectively, and rise to 204, 139, and 99 days considering theoretical minimum-risk concentrations.

In response to the relatively high pollution concentrations and frequent pollution exceedance, Asia and Africa witness the largest mortality rate in health burden (Fig. 2a), particularly from PM<sub>2.5</sub> pollution. For instance, South Asia exhibits 18.2 (95% CI: 12.2–24.3) mortality per 100k population, East Asia 15.8 (10.4–21.5), and Western Sub-Saharan Africa 15.5 (10.1–20.1). PM<sub>2.5</sub> also strongly affects Europe and Latin America (reaching up to 7.5 [95% CI: 4.6–10.7] mortality per 100k population in Central Europe), where NO<sub>2</sub>-related health outcomes are evident as well (up to 4.0 [3.4–4.7] mortality per 100k population in Southern Latin America). In addition to PM<sub>2.5</sub> and NO<sub>2</sub>, O<sub>3</sub> pollution adds significant challenges for high-income regions, such as High Income Asia Pacific of 15.5 (95% CI: 12.6–18.7) mortality per 100k population, Western Europe 7.8 (5.2–11.2), and High Income North America 6.6 (4.6–8.9).

Soil NO<sub>x</sub> emissions contribute 1.3 ± 1.1, 6.3 ± 5.1, and 10.0 ± 8.1% on average to the global health burden attributable to short-term PM<sub>2.5</sub>, O<sub>3</sub>, and NO<sub>2</sub> exposure, respectively (Figure S8), depending on the location and intensity of agricultural activities. South Asia tops the list of the soil NO<sub>x</sub>-related mortality rates, with strong influences from all three pollutants (Fig. 1b,d,f and Fig. 2b), namely 0.60 (95% CI: 0.41–0.81) mortality per 100k population for PM<sub>2.5</sub>, 0.63 (0.46–0.81) for O<sub>3</sub>, and 0.34 [0.24–0.44] for NO<sub>2</sub>. In other regions, the health concerns related to soil NO<sub>x</sub> emissions are predominantly associated with O<sub>3</sub> pollution, with mortality rates reaching up to 0.68 (95% CI: 0.44–0.97) per 100k population in Western Sub-Saharan Africa. This is followed by NO<sub>2</sub>-related impacts, with mortality rates up to 0.28 (95% CI: 0.23–0.33) in Southern Latin America, and PM<sub>2.5</sub>-related impacts, up to 0.20 (0.13–0.27) in East Asia.

#### 3.2. Seasonal variations of soil NO<sub>x</sub>-related health burden

In absolute terms, soil NO<sub>x</sub> contributions to short-term PM<sub>2.5</sub>, O<sub>3</sub>, and NO<sub>2</sub> pollution lead to 13.9 (95% CI: 9.1–18.8), 26.0 (18.2–34.2), and 13.9 (10.3–17.5) thousand mortality, respectively, 2019. The overall health risk peaks in May, a typical sowing and growing period in the Northern Hemisphere, but shows distinct variations across regions, seasons, and pollutants (Fig. 3). Taking South Asia, which accounts for 45.3% of global soil NO<sub>x</sub> attributable mortality, as an example, O<sub>3</sub> poses the most urgent threat to soil NO<sub>x</sub>-related health concerns during warm seasons from March to August, with mortality reaching up to 2.1 (95% CI: 1.5–2.7) thousand per month. In contrast, PM<sub>2.5</sub> attributable mortality is prominent during cold months from September to February, up to 1.4 (95% CI: 0.94–1.8) thousand mortality per month.

A similar dominant role of O<sub>3</sub> pollution is detected in East Asia during summer, whereas NO<sub>2</sub>-related health effects become the most pronounced in the cold months. More complexly, in May, a co-pollutant-driven health concern is noticed, with mortality of 459 (95% CI: 298–625) for PM<sub>2.5</sub>, 468 (339–603) for O<sub>3</sub>, and 520 (406–634) for NO<sub>2</sub>. The abovementioned seasonal variations in South Asia and East Asia,

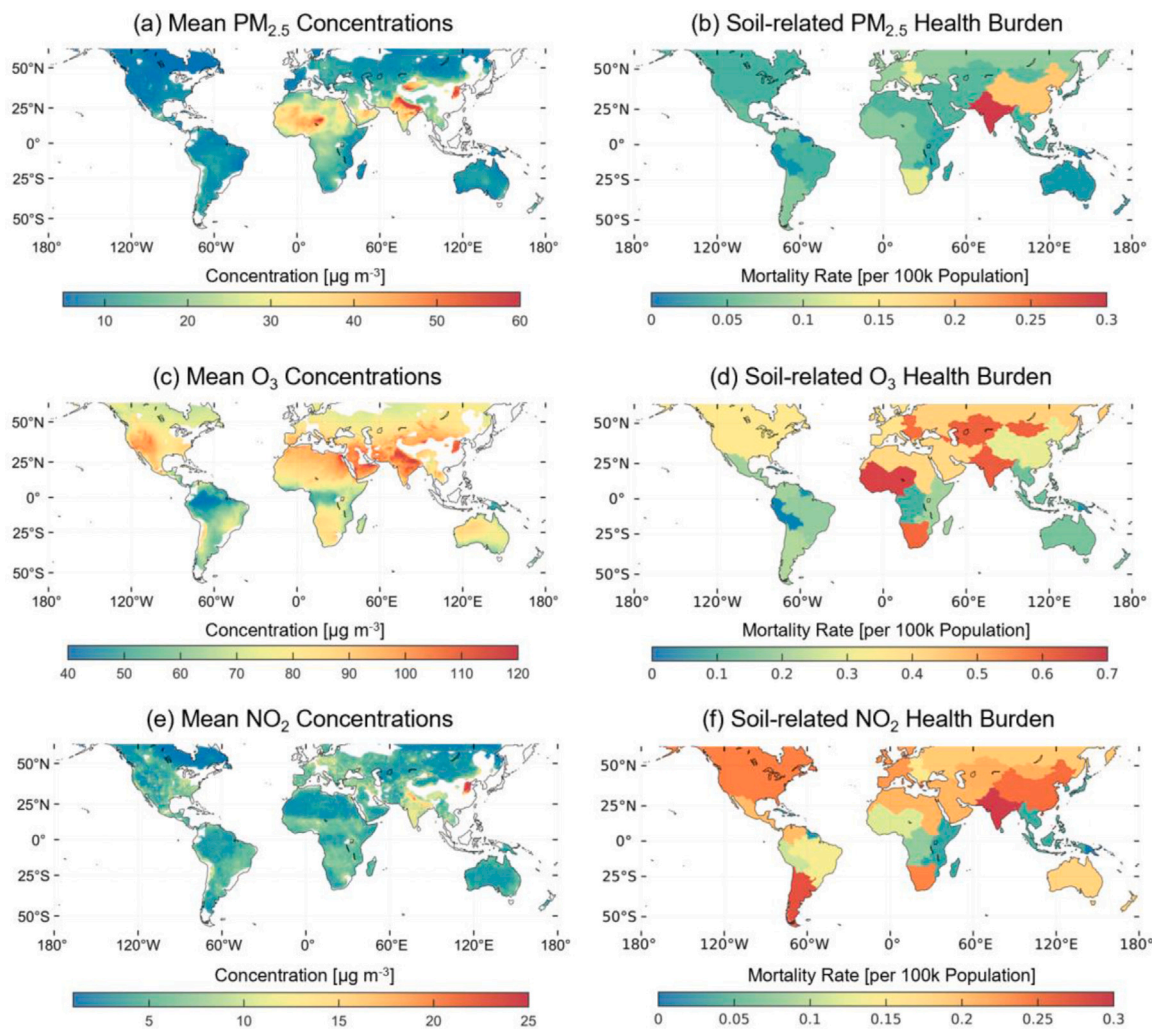


**Fig. 1.** Mean values of daily PM<sub>2.5</sub>, daily maximum 8-h average (MDA8) O<sub>3</sub>, and daily NO<sub>2</sub> concentrations and acute mortality rates contributed by soil NO<sub>x</sub> emissions in 2019. Concentrations with low influences from soil NO<sub>x</sub> (fractions of soil NO<sub>x</sub> emissions to NO<sub>2</sub> concentrations lower than 30% for all months) ([Vinken et al., 2014](#)) are not shown. (For interpretation of the references to color in this figure legend, the reader is referred to the web version of this article.)

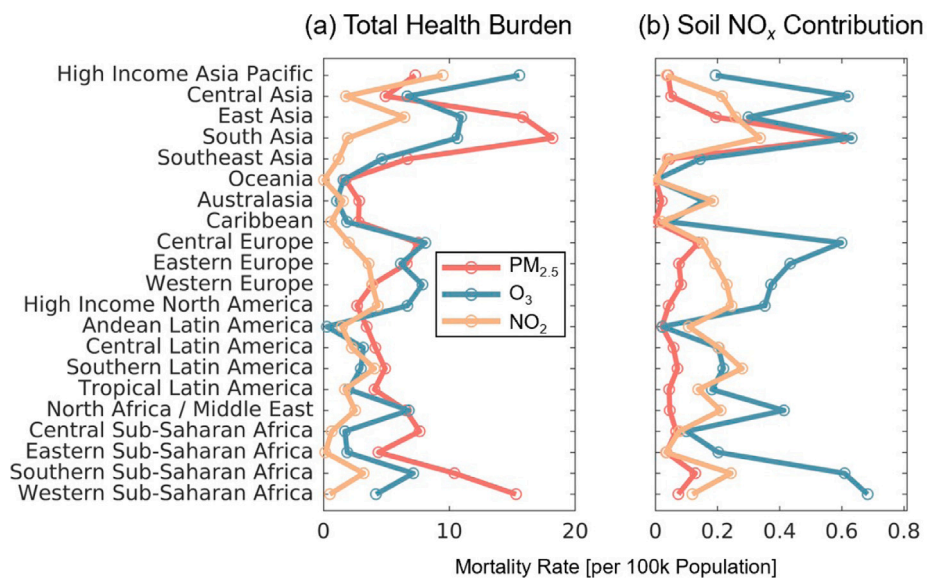


**Fig. 2.** Region-level health burden related to short-term exposure of PM<sub>2.5</sub>, O<sub>3</sub>, and NO<sub>2</sub> in 2019 and contributions of soil NO<sub>x</sub> emissions. (For interpretation of the references to color in this figure legend, the reader is referred to the web version of this article.)

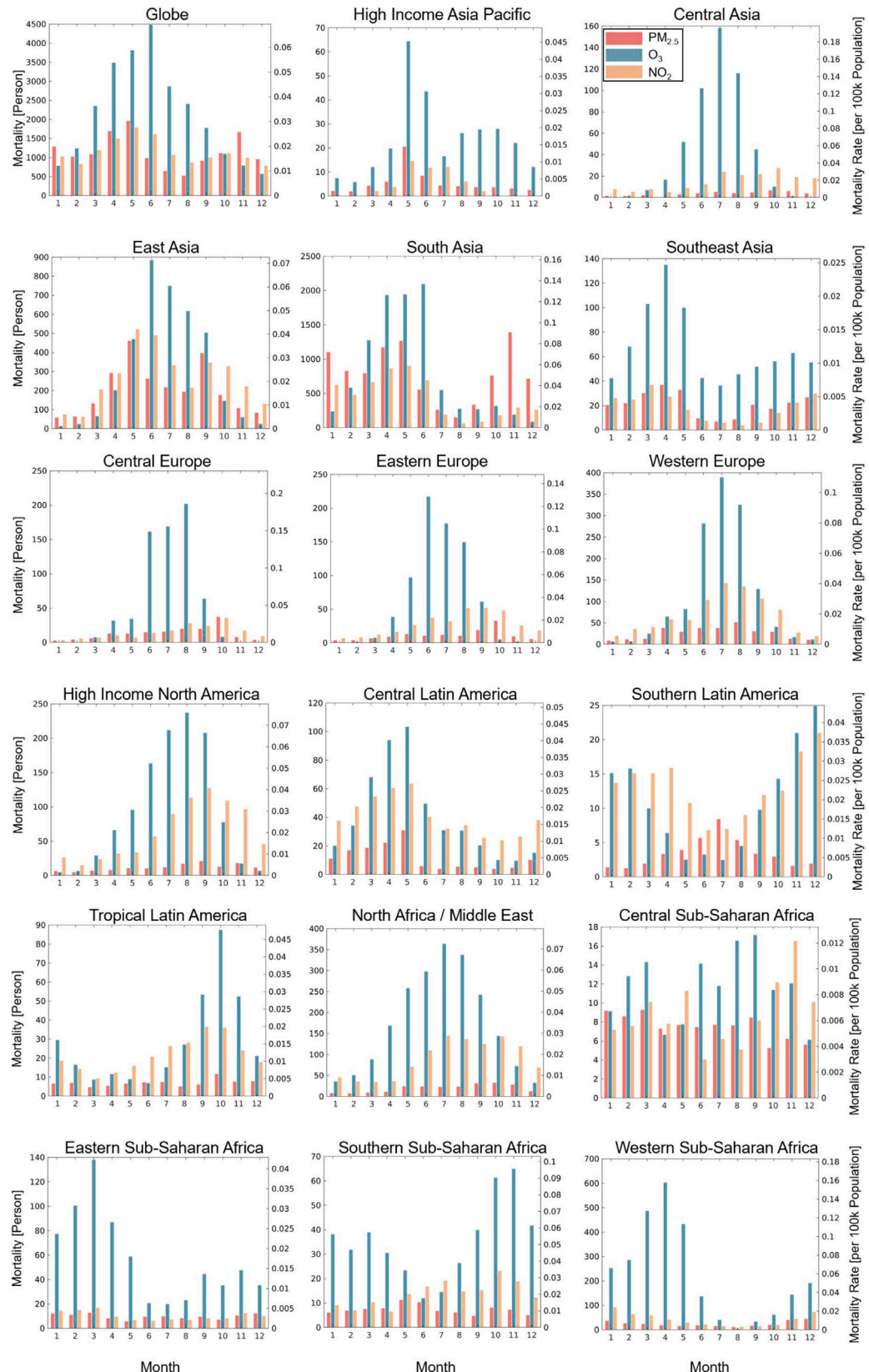


**Fig. 3.** Monthly variations of soil NO<sub>x</sub> contributions to the acute health burden of PM<sub>2.5</sub>, O<sub>3</sub>, and NO<sub>2</sub>. Results are only shown for regions with maximum monthly mortality larger than 10. (For interpretation of the references to color in this figure legend, the reader is referred to the web version of this article.)

influenced by the combined effects of health burden (Figure S9) and soil  $\text{NO}_x$  contributions (Figure S8), differ from the patterns of pollution concentrations or soil  $\text{NO}_x$  emissions reported in other studies (Shen et al., 2022; Ding et al., 2022). This underscores the complexity of health management and the necessity of source attribution.

Looking beyond South Asia and East Asia, soil  $\text{NO}_x$ -contributed  $\text{O}_3$  pollution broadly concerns public health during growing seasons and warm months, with region-dependent peaks of up to 603 (95% CI: 406–810) mortality per month. These peaks occur at different times, for instance, March in Eastern Sub-Saharan Africa, April in West Sub-Saharan Africa, May in Central Latin America, June in Eastern Europe, July in Western Europe, and August in High Income North America. During cold months, although soil  $\text{NO}_x$  contributions are typically less than 15% (Figure S8), the health burden from short-term  $\text{NO}_2$  exposure remains significant, with regional mortality of up to 142 (95% CI: 113–172) per month, particularly evident in Central Asia, High Income North America, Central Latin America, North Africa/Middle East, and across Europe.

Despite our focus on the soil  $\text{NO}_x$  influences, it is important to highlight the significant health burden attributable to short-term  $\text{PM}_{2.5}$  exposure from all sources, which amounts to 716.2 (95% CI: 466.7–973.1) thousand mortality globally. This burden is considerably higher compared to  $\text{O}_3$  (500.3 [95% CI: 352.5–654.7] thousand) and  $\text{NO}_2$  (198.2 [155.8–541.2] thousand), especially during winter (Figure S9). The remaining agriculture-originated  $\text{PM}_{2.5}$  sources include direct emissions from agricultural waste burning (Lan et al., 2022) and secondary formation from ammonia, another prevalent atmospheric pollutant released from fertilizer use (Pozzer et al., 2017).

### 3.3. Correlation between soil and anthropogenic sources

The management of pollution attributable health outcomes is complicated by the correlation and interaction effects between soil and anthropogenic sources. In Fig. 4, the comparison between daily mortality caused by soil and anthropogenic  $\text{NO}_x$  emissions reveals broadly negative (and occasionally insignificant) correlations for regions exposed to  $\text{NO}_2$  pollution in cold seasons, such as High Income North America and Europe with values ranging between -0.79 and -0.95. Conversely, correlations are positive (or insignificant) for regions with  $\text{PM}_{2.5}$ -associated health risks, such as East Asia (0.63) and South Asia (0.15), as confirmed by the temporal variations of soil and anthropogenic source fractions in Figures S8 and S10.

With an increased heterogeneity,  $\text{O}_3$  is generally linked with positive correlations in warm months reaching up to 0.85 over middle to high latitudes (e.g., East Asia, Western Europe, and High Income North America) and negative values of up to -0.82 over low latitudes (e.g., Western Sub-Saharan Africa). Differences in (anti-)correlations highlight the temporal and spatial dynamics of local  $\text{NO}_x$  sources and their relative significance in the context of health management. Notably, the positive correlations can be biased, as our zeroing-out method quantifies the actual impact of sources on health burden, including pure influence and the non-linear interaction with all other sources (Li et al., 2018). Such analysis of responses and correlations will be further benefited from sensitivity simulations with each source perturbed (instead of turned off).

In light of policy planning, the importance of soil  $\text{NO}_x$  emissions is particularly distinct for regions where anthropogenic and soil sources are negatively correlated and well separated spatially or temporally. These regions warrant a dynamically targeted control strategy to prioritize limited resources for effective actions. Meanwhile, a synergistic control strategy for positively correlated regions is needed to incorporate the intrinsic linkage and interactions between anthropogenic and soil sources. In particular, the recognized emission control penalty effect in the presence of large soil  $\text{NO}_x$  emissions necessitates a more stringent reduction of anthropogenic emissions to achieve the  $\text{O}_3$  control targets (Lu et al., 2021). Regardless of the correlation type, improvements in fertilizer use present potential research and regulation directions.

### 3.4. Fertilizer improvement for emission control and health management

As fertilizer usage and soil emissions are expected to increase under the ever-warming climate (Xu et al., 2024; Quan et al., 2024), and given that large-scale climatic conditions are comparatively difficult to alter in practice, the priority to alleviate health risks of soil  $\text{NO}_x$ -originated pollution lies in the sustainable application of nitrogen (N) fertilizers. In Fig. 5, synthetic N fertilizers with surface placement are intensively applied globally in 2019, with the widely used urea standing out as the top place (average application rate of  $430.5 \pm 241.7 \text{ kg N ha}^{-1}$ ), followed by N-P-K compound fertilizer ( $148.9 \pm 231.2 \text{ kg N ha}^{-1}$ ) and ammonium nitrate fertilizer ( $100.4 \pm 121.4 \text{ kg N ha}^{-1}$ ). The intensive use of fertilizers is typically accompanied by high soil  $\text{NO}_x$ -related health concerns, especially for developing regions or agriculturally intensive areas.

Ammonium nitrate fertilizer, which typically results in significant increases in soil  $\text{NO}_x$  emissions (59% compared to 40% for urea and 20% for organic fertilizers) (Liu et al., 2017), is primarily used in Europe, with application rates of up to  $363.6 \text{ kg N ha}^{-1}$  in Central Europe. Meanwhile, populated Asia is characterized by the most intensive use of compound fertilizers (up to  $975.1 \text{ kg N ha}^{-1}$  for N-P-K compound in East Asia), particularly with surface placement that potentially leads to an imbalance between fertilizer supply and crop demand.

In contrast, a deep use (a fertilizer application method with a high N use efficiency) (Zhu et al., 2024) of liquid fertilizers (a fertilizer type rich in N content) (Pan et al., 2022) is predominantly observed in Europe and the Americas, with application rates of up to  $340.6 \text{ kg N ha}^{-1}$  for N solutions and  $311.9 \text{ kg N ha}^{-1}$  for anhydrous ammonia in High Income North America. This fertilizer use presents an attractive measure to address global air pollution and health concerns. Such improvements in agricultural management are urgently needed, as existing cropland is projected to intensify with the growing population and increasing food demand (Bodirsky et al., 2014). Consequently, the application rate of synthetic N fertilizers is expected to rise, exacerbating soil  $\text{NO}_x$  emissions (Yao et al., 2017).

Despite the variable fertilizer requirements for different crop types, soil characteristics, yield expectations, and meteorological or climatic factors, there exist several potential management practices to realize proper fertilization application and increased N use efficiency (Pan et al., 2022), such as improving N application method (e.g., deep placement instead of surface placement for urea) (Hou et al., 2010), changing N formulation (e.g., liquid or suspension formulation instead of granulation for N-P-K compound) (Yahaya et al., 2023), substituting synthetic N fertilizer with (bio-)organic fertilizers (Geng et al., 2021), applying slow- or controlled-release fertilizers (Cheng et al., 2002) and nitrification inhibitors (Wang et al., 2021a), and innovating farmland techniques (e.g., adjusted fertilizer rate to meet plant demand) (Yadav et al., 2017).

Encouragingly, integrating the aforementioned practices to mitigate soil  $\text{NO}_x$  emissions from agricultural activities is gaining more attention. For instance, the EU's Farm to Fork strategy includes fertilizer-related targets of decreasing nutrient loss by 50%, reducing fertilizer use by 20%, and increasing the share of organic farming by 25% by 2030 (European Commission, 2020). Similar strategies and goals have also been proposed by policy-makers worldwide, such as the Technical Guidelines for Green Agricultural Development (2018–2030) in China and the Green-Ag project in India. Additional quantitative insights regarding soil  $\text{NO}_x$  emissions and health burden can be gained from perturbation simulations with updated chemical fertilizer application inventory in BDSNP. Nevertheless, our qualitative analysis should not downplay the significance of findings in terms of policy implications.

Farmland management measures are crucial for developing regions or agricultural areas experiencing significant health risks, such as South Asia, Southern Sub-Saharan Africa, and Central Europe. These regions rank among the highest for soil  $\text{NO}_x$ -related health burden with up to 1.6 (95% CI: 1.1–2.1) mortality per 100k population and rely

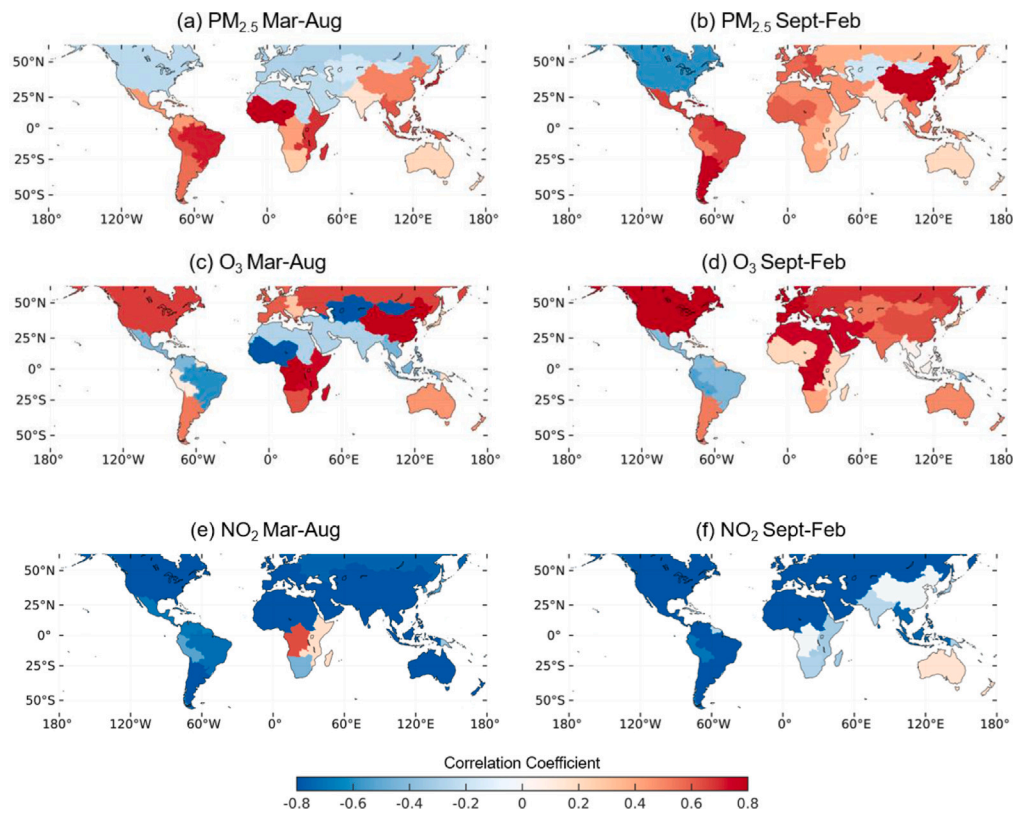


**Fig. 4.** Correlation coefficients between daily percentage contributions of soil and anthropogenic  $\text{NO}_x$  emissions to the acute health burden of  $\text{PM}_{2.5}$ ,  $\text{O}_3$ , and  $\text{NO}_2$  in March to August (warm seasons in the Northern Hemisphere) and September to February (cold seasons in the Northern Hemisphere). (For interpretation of the references to color in this figure legend, the reader is referred to the web version of this article.)

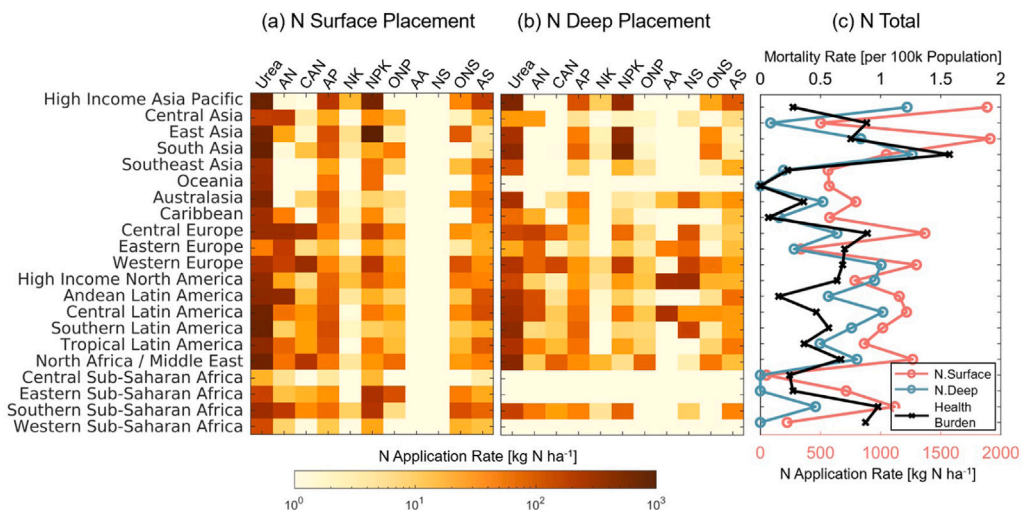


**Fig. 5.** Average cropland application rate of synthetic nitrogen (N) fertilizers in 2019, including urea, nitrate fertilizers, compound fertilizers, liquid fertilizers, and other synthetic fertilizers. Nitrate fertilizers include ammonium nitrate (AN) and calcium ammonium nitrate (CAN). Compound fertilizers include ammonium phosphate (AP), N-K compounds (NK), N-P-K compounds (NPK), and other NP (ONP). Liquid fertilizers include anhydrous ammonia (AA) and N solutions (NS). Other synthetic fertilizers include other N straight (ONS) and ammonium sulphate (AS). Soil  $\text{NO}_x$ -related health burden (sum of values for  $\text{PM}_{2.5}$ ,  $\text{O}_3$ , and  $\text{NO}_2$  exposure) is also shown. Fertilizer data are taken from <https://doi.org/10.11888/Terre.tpd.300446>. (For interpretation of the references to color in this figure legend, the reader is referred to the web version of this article.)

substantially on synthetic N fertilizers, including urea (up to 28.9% of all N fertilizer types), nitrate (29.3%), and compound (26.2%) fertilizers (Fig. 5). Seasonally, farmland management measures shall be implemented not only during growing and warm seasons to mitigate  $\text{O}_3$ -related health risks but also during cold months for regions where

$\text{NO}_2$  or  $\text{PM}_{2.5}$  exposure poses major health concerns. Particularly in areas with considerable all-sourced  $\text{PM}_{2.5}$  attributable health burden, such as Asia and Africa, coordinated fertilizer improvements are needed to achieve balanced emission reductions of  $\text{NO}_x$  and ammonia (Pan et al., 2022).

#### 4. Conclusions

In this study, we analyze sectoral impacts from soil NO<sub>x</sub> emissions on PM<sub>2.5</sub>, O<sub>3</sub>, and NO<sub>2</sub>-attributable health burden by integrating machine-leaning-based daily exposure estimates, GEOS-Chem model sensitivity simulations, and short-term exposure-response functions. In 2019, 72.3% of the globe is affected by soil NO<sub>x</sub> emissions, whose contributions to short-term PM<sub>2.5</sub>, O<sub>3</sub>, and NO<sub>2</sub> pollution result in 13.9 (95% CI: 9.1–18.8), 26.0 (18.2–34.2), and 13.9 (10.3–17.5) thousand premature mortality, respectively. Soil NO<sub>x</sub>-originated air pollution poses a global health concern, with distinct variations in regions, seasons, and pollutants. Regionally, South Asia, Southern Sub-Saharan Africa, and Central Europe with intensive fertilizer use witness the largest soil NO<sub>x</sub>-related health burden of up to 1.6 (95% CI: 1.1–2.1) mortality per 100k population. Seasonally, the overall health risk peaks in May, with O<sub>3</sub> pollution typically dominating the soil NO<sub>x</sub>-attributable health burden during warm seasons and NO<sub>2</sub> or PM<sub>2.5</sub> during cold months.

This work emphasizes the region- and season-dependent importance of soil NO<sub>x</sub> for emission control and health benefits, particularly for developing regions and intensively agricultural areas, which will become increasingly prominent under effective regulation of combustion emissions. Such insights from a global perspective are crucial to customize strategic policies with the greatest public health benefits. In light of policy making, farmland management measures to realize proper synthetic fertilizer application and increased N use efficiency offer achievable solutions to alleviate health risks of soil NO<sub>x</sub>-originated pollution. These agricultural policies can be additionally complicated by the (anti-)correlations between soil and anthropogenic sources, requiring a (targeted) synergistic control strategy under the ever-changing climate. In the future, the potential health benefits achievable from fertilizer improvements will be estimated using updated knowledge of soil nitrogen content, and the intrinsic links and trade-off practices among fertilizer improvement, economic cost, food production, O<sub>3</sub> formation regime, and meteorological and climate change still require further analysis.

Uncertainties remain in our conclusions upon the integration of exposure estimates, model simulations, and health risks. First, the zeroing-out method considers both the pure contributions of soil NO<sub>x</sub> alone and interactional effects with all other sectors, particularly for O<sub>3</sub>, due to the non-linear compensating effects among different sources (Li et al., 2018; Lu et al., 2021). Such method, focusing on impacts (source sensitivities), can be combined with the tagging approach, focusing on contributions (source apportionments), to reveal how the contribution of sectoral sources to pollutant changes in response to mitigation measures (Butler et al., 2020; Gao et al., 2020; Li et al., 2023b). Second, our region-scale analysis may be limited by the spatial resolution of GEOS-Chem simulations (Weng et al., 2020), and future country- or city-scale studies will benefit from high-resolution nested simulations. Third, our estimates of health burden are expected to be higher than previous regional studies (by 1.8 times) (Xiao et al., 2021; Wang et al., 2021c), due to the use of relatively strict theoretical minimum-risk concentrations and high relative risk. For local emission control and health management, such global-friendly parameters can be improved with age-, source-, and country-specific epidemiologic studies (Chen et al., 2017; Yin et al., 2017; Nan et al., 2023).

#### CRediT authorship contribution statement

**Song Liu:** Writing – review & editing, Writing – original draft, Methodology, Investigation, Formal analysis, Conceptualization. **Jing Wei:** Writing – review & editing, Methodology, Investigation, Data curation. **Xicheng Li:** Writing – review & editing, Resources, Data curation. **Lei Shu:** Writing – review & editing, Validation, Investigation. **Jiaming Zhang:** Writing – review & editing, Resources. **Tzung-May Fu:** Writing – review & editing, Supervision, Funding acquisition. **Xin Yang:** Writing – review & editing, Supervision, Funding acquisition. **Lei Zhu:** Writing – review & editing, Writing – original draft, Supervision, Methodology, Funding acquisition, Conceptualization.

#### Declaration of competing interest

The authors declare that they have no known competing financial interests or personal relationships that could have appeared to influence the work reported in this paper.

#### Acknowledgments

This work is funded by the National Natural Science Foundation of China (42205134, 42375090), Shenzhen Key Laboratory of Precision Measurement and Early Warning Technology for Urban Environmental Health Risks, China (ZDSYS20220606100604008), Guangdong Basic and Applied Basic Research Foundation, China (2024A1515011951, 2021A1515110713), Guangdong University Research Project Science Team, China (2021KCXTD004), Major Talent Project of Guangdong Province, China (2021QN020924), Shenzhen Science and Technology Program, China (KQTD20210811090048025, JCYJ2022053011540409), and High level of special funds, China (G03050K001). This work is supported by the Center for Computational Science and Engineering at Southern University of Science and Technology, China.

#### Appendix A. Supplementary data

Supplementary material related to this article can be found online at <https://doi.org/10.1016/j.envint.2024.109087>.

#### Data availability

Data will be made available on request.

#### References

- Adalibieke, W., Cui, X., Cai, H., You, L., Zhou, F., 2023. Global crop-specific nitrogen fertilization dataset in 1961–2020. *Sci. Data* 10 (1), 617.
- Anenberg, S.C., Horowitz, L.W., Tong, D.Q., West, J.J., 2010. An estimate of the global burden of anthropogenic ozone and fine particulate matter on premature human mortality using atmospheric modeling. *Environ. Health Perspect.* 118 (9), 1189–1195.
- Bodirsky, B.L., Popp, A., Lotze-Campen, H., Dietrich, J.P., Rolinski, S., Weindl, I., Schmitz, C., Müller, C., Bonsch, M., Humpenöder, F., Biewald, A., Stevanovic, M., 2014. Reactive nitrogen requirements to feed the world in 2050 and potential to mitigate nitrogen pollution. *Nature Commun.* 5 (1), 3858.
- Boersma, K., Jacob, D.J., Trainic, M., Rudich, Y., DeSmedt, I., Dirksen, R., Eskes, H., 2009. Validation of urban NO<sub>2</sub> concentrations and their diurnal and seasonal variations observed from the SCIAMACHY and OMI sensors using in situ surface measurements in Israeli cities. *Atmos. Chem. Phys.* 9 (12), 3867–3879.
- Butler, T., Lupascu, A., Nalam, A., 2020. Attribution of ground-level ozone to anthropogenic and natural sources of nitrogen oxides and reactive carbon in a global chemical transport model. *Atmos. Chem. Phys.* 20 (17), 10707–10731.
- Chen, R., Yin, P., Meng, X., Liu, C., Wang, L., Xu, X., Ross, J.A., Tse, L.A., Zhao, Z., Kan, H., Zhou, M., 2017. Fine particulate air pollution and daily mortality. A nationwide analysis in 272 Chinese cities. *Am. J. Respir. Crit. Care Med.* 196 (1), 73–81.
- Cheng, W., Nakajima, Y., Sudo, S., Akiyama, H., Tsuruta, H., 2002. N<sub>2</sub>O and NO emissions from a field of Chinese cabbage as influenced by band application of urea or controlled-release urea fertilizers. *Nutr. Cycl. Agroecosyst.* 63, 231–238.
- David, L.M., Ravishankara, A., Brewer, J.F., Sauvage, B., Thouret, V., Venkataramani, S., Sinha, V., 2019. Tropospheric ozone over the Indian subcontinent from 2000 to 2015: Data set and simulation using GEOS-Chem chemical transport model. *Atmos. Environ.* 219, 117039.
- Dedoussi, I.C., Eastham, S.D., Monier, E., Barrett, S.R., 2020. Premature mortality related to United States cross-state air pollution. *Nature* 578 (7794), 261–265.
- Ding, J., van der A, R., Mijling, B., de Laat, J., Eskes, H., Boersma, K.F., 2022. NO<sub>x</sub> emissions in India derived from OMI satellite observations. *Atmospheric Environ.* X 14, 100174.
- European Commission, 2020. A farm to fork strategy for a fair, healthy and environmentally-friendly food system. COM(2020)381.
- Fritz, T.M., Eastham, S.D., Emmons, L.K., Lin, H., Lundgren, E.W., Goldhaber, S., Barrett, S.R.H., Jacob, D.J., 2022. Implementation and evaluation of the GEOS-Chem chemistry module version 13.1.2 within the Community Earth System Model v2.1. *Geosci. Model Dev.* 15 (23), 8669–8704.

- Gao, M., Gao, J., Zhu, B., Kumar, R., Lu, X., Song, S., Zhang, Y., Jia, B., Wang, P., Beig, G., Hu, J., Ying, Q., Zhang, H., Sherman, P., McElroy, M.B., 2020. Ozone pollution over China and India: seasonality and sources. *Atmos. Chem. Phys.* 20 (7), 4399–4414.
- GBD 2021 Risk Factors Collaborators, 2024. Global burden and strength of evidence for 88 risk factors in 204 countries and 811 subnational locations, 1990–2021: a systematic analysis for the Global Burden of Disease Study 2021. *Lancet* 403 (10440), 2162–2203.
- Garlo, R., McCarty, W., Suárez, M.J., Todling, R., Molod, A., Takacs, L., Randles, C.A., Darmenov, A., Bosilovich, M.G., Reichle, R., Wargan, K., Coy, L., Cullather, R., Draper, C., Akella, S., Buchard, V., Conaty, A., da Silva, M., Gu, W., Kim, G.K., Koster, R., Lucchesi, R., Merkova, D., Nielsen, J.E., Partyka, G., Pawson, S., Putman, W., Rienecker, M., Schubert, S.D., Sienkiewicz, M., Zhao, B., 2017. The modern-era retrospective analysis for research and applications, version 2 (MERRA-2). *J. Clim.* 30 (14), 5419–5454.
- Geng, Y., Yuan, Y., Miao, Y., Zhi, J., Huang, M., Zhang, Y., Wang, H., Shen, Q., Zou, J., Li, S., 2021. Decreased nitrous oxide emissions associated with functional microbial genes under bio-organic fertilizer application in vegetable fields. *Pedosphere* 31 (2), 279–288.
- Geurts, P., Ernst, D., Wehenkel, L., 2006. Extremely randomized trees. *Mach. Learn.* 63, 3–42.
- Giani, P., Anav, A., De Marco, A., Feng, Z., Crippa, P., 2020. Exploring sources of uncertainty in premature mortality estimates from fine particulate matter: the case of China. *Environ. Res. Lett.* 15 (6), 064027.
- Giglio, L., Randerson, J.T., Van Der Werf, G.R., 2013. Analysis of daily, monthly, and annual burned area using the fourth-generation global fire emissions database (GFED4). *J. Geophys. Res. Biogeosci.* 118 (1), 317–328.
- Guenther, A., Jiang, X., Heald, C.L., Sakulyanontvittaya, T., Duhl, T., Emmons, L., Wang, X., 2012. The Model of Emissions of Gases and Aerosols from Nature version 2.1 (MEGAN2.1): an extended and updated framework for modeling biogenic emissions. *Geosci. Model Dev.* 5 (6), 1471–1492.
- Heald, C.L., Geddes, J.A., 2016. The impact of historical land use change from 1850 to 2000 on secondary particulate matter and ozone. *Atmos. Chem. Phys.* 16 (23), 14997–15010.
- Hoesly, R.M., Smith, S.J., Feng, L., Klimont, Z., Janssens-Maenhout, G., Pitkanen, T., Seibert, J.J., Vu, L., Andres, R.J., Bolt, R.M., Bond, T.C., Dawidowski, L., Kholod, N., Kurokawa, J.-I., Li, M., Liu, L., Lu, Z., Moura, M.C.P., O'Rourke, P.R., Zhang, Q., 2018. Historical (1750–2014) anthropogenic emissions of reactive gases and aerosols from the Community Emissions Data System (CEDS). *Geosci. Model Dev.* 11 (1), 369–408.
- Hou, A., Tsuruta, H., McCREARY, M.A., Hosen, Y., 2010. Effect of urea placement on the time-depth profiles of NO, N<sub>2</sub>O and mineral nitrogen concentrations in an Andisol during a Chinese cabbage growing season. *Soil Sci. Plant Nutr.* 56 (6), 861–869.
- Huang, L., Fang, J., Liao, J., Yarwood, G., Chen, H., Wang, Y., Li, L., 2023. Insights into soil NO emissions and the contribution to surface ozone formation in China. *Atmos. Chem. Phys.* 23 (23), 14919–14932.
- Huber, D.E., Steiner, A.L., Kort, E.A., 2020. Daily cropland soil NO<sub>x</sub> emissions identified by TROPOMI and SMAP. *Geophys. Res. Lett.* 47 (22), e2020GL089949.
- Huber, D.E., Steiner, A.L., Kort, E.A., 2023. Sensitivity of modeled soil NO<sub>x</sub> emissions to soil moisture. *J. Geophys. Res.: Atmos.* 128 (7), e2022JD037611.
- Hudman, R., Moore, N., Mebust, A., Martin, R., Russell, A., Valin, L., Cohen, R., 2012. Steps towards a mechanistic model of global soil nitric oxide emissions: implementation and space based-constraints. *Atmos. Chem. Phys.* 12 (16), 7779–7795.
- Keller, C.A., Long, M.S., Yantosca, R.M., Da Silva, A., Pawson, S., Jacob, D.J., 2014. HEMCO v1.0: a versatile, ESMF-compliant component for calculating emissions in atmospheric models. *Geosci. Model Dev.* 7 (4), 1409–1417.
- Lan, R., Eastham, S.D., Liu, T., Norford, L.K., Barrett, S.R., 2022. Air quality impacts of crop residue burning in India and mitigation alternatives. *Nature Commun.* 13 (1), 6537.
- Lelieveld, J., Barlas, C., Giannadaki, D., Pozzer, A., 2013. Model calculated global, regional and megacity premature mortality due to air pollution. *Atmos. Chem. Phys.* 13 (14), 7023–7037.
- Lelieveld, J., Evans, J., Fnais, M., Giannadaki, D., Pozzer, A., 2015. The contribution of outdoor air pollution sources to premature mortality on a global scale. *Nature* 525 (7569), 367–371.
- Li, N., He, Q., Greenberg, J., Guenther, A., Li, J., Cao, J., Wang, J., Liao, H., Wang, Q., Zhang, Q., 2018. Impacts of biogenic and anthropogenic emissions on summertime ozone formation in the Guanzhong Basin, China. *Atmos. Chem. Phys.* 18 (10), 7489–7507.
- Li, C., van Donkelaar, A., Hammer, M.S., McDuffie, E.E., Burnett, R.T., Spadaro, J.V., Chatterjee, D., Cohen, A.J., Apte, J.S., Southerland, V.A., Anenberg, S.C., Brauer, M., Martin, R.V., 2023a. Reversal of trends in global fine particulate matter air pollution. *Nature Commun.* 14 (1), 5349.
- Li, P., Yang, Y., Wang, H., Li, S., Li, K., Wang, P., Li, B., Liao, H., 2023b. Source attribution of near-surface ozone trends in the United States during 1995–2019. *Atmos. Chem. Phys.* 23 (9), 5403–5417.
- Liu, S., Li, X., Li, J., Shu, L., Fu, T.M., Yang, X., Zhu, L., 2023. Observing network effect of shipping emissions from space: A natural experiment in the world's busiest port. *PNAS Nexus* 2 (11), pgad391.
- Liu, S., Li, X., Wei, J., Shu, L., Jin, J., Fu, T.M., Yang, X., Zhu, L., 2024. Short-term exposure to fine particulate matter and ozone: Source impacts and attributable mortalities. *Environ. Sci. Technol.* 58 (26), 11256–11267.
- Liu, S., Lin, F., Wu, S., Ji, C., Sun, Y., Jin, Y., Li, S., Li, Z., Zou, J., 2017. A meta-analysis of fertilizer-induced soil NO and combined NO+N<sub>2</sub>O emissions. *Global Change Biol.* 23 (6), 2520–2532.
- Lu, X., Ye, X., Zhou, M., Zhao, Y., Weng, H., Kong, H., Li, K., Gao, M., Zheng, B., Lin, J., Zhou, F., Zhang, Q., Wu, D., Zhang, L., Zhang, Y., 2021. The underappreciated role of agricultural soil nitrogen oxide emissions in ozone pollution regulation in North China. *Nature Commun.* 12 (1), 5021.
- Lyu, X., Li, K., Guo, H., Morawska, L., Zhou, B., Zeren, Y., Jiang, F., Chen, C., Goldstein, A.H., Xu, X., Wang, T., Lu, X., Zhu, T., Querol, X., Chatani, S., Latif, M.T., Schuch, D., Sinha, V., Kumar, P., Mullins, B., Seguel, R., Shao, M., Xue, L., Wang, N., Chen, J., Gao, J., Chai, F., Simpson, I., Sinha, B., Blake, D.R., 2023. A synergistic ozone-climate control to address emerging ozone pollution challenges. *One Earth* 6 (8), 964–977.
- McDuffie, E.E., Martin, R.V., Spadaro, J.V., Burnett, R., Smith, S.J., O'Rourke, P., Hammer, M.S., van Donkelaar, A., Bindle, L., Shah, V., Jaeglé, L., Luo, G., Yu, F., Adeniran, J.A., Lin, J., Brauer, M., 2021. Source sector and fuel contributions to ambient PM<sub>2.5</sub> and attributable mortality across multiple spatial scales. *Nature Commun.* 12 (1), 3594.
- Miyazaki, K., Eskes, H., Sudo, K., Boersma, K.F., Bowman, K., Kanaya, Y., 2017. Decadal changes in global surface NO<sub>x</sub> emissions from multi-constituent satellite data assimilation. *Atmos. Chem. Phys.* 17 (2), 807–837.
- Nan, N., Yan, Z., Zhang, Y., Chen, R., Qin, G., Sang, N., 2023. Overview of PM<sub>2.5</sub> and health outcomes: focusing on components, sources, and pollutant mixture co-exposure. *Chemosphere* 323, 138181.
- Orellano, P., Reynoso, J., Quaranta, N., Bardach, A., Ciapponi, A., 2020. Short-term exposure to particulate matter (PM<sub>10</sub> and PM<sub>2.5</sub>), nitrogen dioxide (NO<sub>2</sub>), and ozone (O<sub>3</sub>) and all-cause and cause-specific mortality: Systematic review and meta-analysis. *Environ. Int.* 142, 105876.
- Pan, S.Y., He, K.H., Lin, K.T., Fan, C., Chang, C.T., 2022. Addressing nitrogenous gases from croplands toward low-emission agriculture. *Npj Clim. Atmospheric Sci.* 5 (1), 43.
- Potter, P., Ramankutty, N., Bennett, E.M., Donner, S.D., 2010. Characterizing the spatial patterns of global fertilizer application and manure production. *Earth Interact.* 14 (2), 1–22.
- Pozzer, A., Tsimplidi, A.P., Karydis, V.A., De Meij, A., Lelieveld, J., 2017. Impact of agricultural emission reductions on fine-particulate matter and public health. *Atmos. Chem. Phys.* 17 (20), 12813–12826.
- Quan, Q., Yi, F., Liu, H., 2024. Fertilizer response to climate change: Evidence from corn production in China. *Sci. Total Environ.* 928, 172226.
- Seinfeld, J.H., Pandis, S.N., 2016. *Atmospheric Chemistry and Physics: from Air Pollution to Climate Change*. John Wiley & Sons.
- Sha, T., Ma, X., Zhang, H., Janechek, N., Wang, Y., Wang, Y., Castro García, L., Jenerette, G.D., Wang, J., 2021. Impacts of soil NO<sub>x</sub> emission on O<sub>3</sub> air quality in Rural California. *Environ. Sci. Technol.* 55 (10), 7113–7122.
- Shen, Y., Xiao, Z., Wang, Y., Xiao, W., Yao, L., Zhou, C., 2023. Impacts of agricultural soil NO<sub>x</sub> emissions on O<sub>3</sub> over Mainland China. *J. Geophys. Res.: Atmos.* 128 (4), e2022JD037986.
- Shen, Y., Xiao, Z., Wang, Y., Yao, L., Xiao, W., 2022. Multisource remote sensing based estimation of soil NO<sub>x</sub> emissions from fertilized cropland at high-resolution: Spatio-temporal patterns and impacts. *J. Geophys. Res.: Atmos.* 127 (20), e2022JD036741.
- Stavrakou, T., Müller, J.-F., Boersma, K.F., De Smedt, I., Van Der A, R., 2008. Assessing the distribution and growth rates of NO<sub>x</sub> emission sources by inverting a 10-year record of NO<sub>2</sub> satellite columns. *Geophys. Res. Lett.* 35 (10).
- Vinken, G., Boersma, K., Maasakers, J., Adon, M., Martin, R., 2014. Worldwide biogenic soil NO<sub>x</sub> emissions inferred from OMI NO<sub>2</sub> observations. *Atmos. Chem. Phys.* 14 (18), 10363–10381.
- Wang, X., Bai, J., Xie, T., Wang, W., Zhang, G., Yin, S., Wang, D., 2021a. Effects of biological nitrification inhibitors on nitrogen use efficiency and greenhouse gas emissions in agricultural soils: A review. *Ecotoxicol. Environ. Safety* 220, 112338.
- Wang, Y., Ge, C., Garcia, L.C., Jenerette, G.D., Oikawa, P.Y., Wang, J., 2021b. Improved modelling of soil NO<sub>x</sub> emissions in a high temperature agricultural region: role of background emissions on NO<sub>2</sub> trend over the US. *Environ. Res. Lett.* 16 (8), 084061.
- Wang, F., Qiu, X., Cao, J., Peng, L., Zhang, N., Yan, Y., Li, R., 2021c. Policy-driven changes in the health risk of PM<sub>2.5</sub> and O<sub>3</sub> exposure in China during 2013–2018. *Sci. Total Environ.* 757, 143775.
- Wang, Y., Wild, O., Chen, X., Wu, Q., Gao, M., Chen, H., Qi, Y., Wang, Z., 2020. Health impacts of long-term ozone exposure in China over 2013–2017. *Environ. Int.* 144, 106030.
- Wei, J., Li, Z., Li, K., Dickerson, R.R., Pinker, R.T., Wang, J., Liu, X., Sun, L., Xue, W., Cribb, M., 2022a. Full-coverage mapping and spatiotemporal variations of ground-level ozone (O<sub>3</sub>) pollution from 2013 to 2020 across China. *Remote Sens. Environ.* 270, 112775.
- Wei, J., Li, Z., Lyapustin, A., Wang, J., Dubovik, O., Schwartz, J., Sun, L., Li, C., Liu, S., Zhu, T., 2023a. First close insight into global daily gapless 1 km PM<sub>2.5</sub> pollution, driving factors, and health impact. *Nature Commun.* 14 (1), 8349.

- Wei, J., Li, Z., Pinker, R.T., Wang, J., Sun, L., Xue, W., Li, R., Cribb, M., 2021. Himawari-8-derived diurnal variations in ground-level PM<sub>2.5</sub> pollution across China using the fast space-time Light Gradient Boosting Machine (LightGBM). *Atmos. Chem. Phys.* 21 (10), 7863–7880.
- Wei, J., Li, Z., Wang, J., Li, C., Gupta, P., Cribb, M., 2023b. Ground-level gaseous pollutants (NO<sub>2</sub>, SO<sub>2</sub>, and CO) in China: Daily seamless mapping and spatiotemporal variations. *Atmospheric Chem. Phys.* 23 (2), 1511–1532.
- Wei, J., Liu, S., Li, Z., Liu, C., Qin, K., Liu, X., Pinker, R.T., Dickerson, R.R., Lin, J., Boersma, K., Sun, L., Li, R., Xue, W., Cui, Y., Zhang, C., Wang, J., 2022b. Ground-level NO<sub>2</sub> surveillance from space across China for high resolution using interpretable spatiotemporally weighted artificial intelligence. *Environ. Sci. Technol.* 56 (14), 9988–9998.
- Weng, H., Lin, J., Martin, R., Millet, D.B., Jaeglé, L., Ridley, D., Keller, C., Li, C., Du, M., Meng, J., 2020. Global high-resolution emissions of soil NO<sub>x</sub>, sea salt aerosols, and biogenic volatile organic compounds. *Sci. Data* 7 (1), 148.
- Xiao, Q., Geng, G., Xue, T., Liu, S., Cai, C., He, K., Zhang, Q., 2021. Tracking PM<sub>2.5</sub> and O<sub>3</sub> pollution and the related health burden in China 2013–2020. *Environ. Sci. Technol.* 55 (11), 6922–6932.
- Xu, P., Li, G., Zheng, Y., Fung, J.C., Chen, A., Zeng, Z., Shen, H., Hu, M., Mao, J., Zheng, Y., Cui, X., Guo, Z., Chen, Y., Feng, L., He, S., Zhang, X., Lau, A.K.H., Tao, S., Houlton, B.Z., 2024. Fertilizer management for global ammonia emission reduction. *Nature* 626 (8000), 792–798.
- Yadav, M., Kumar, R., Parihar, C., Yadav, R., Jat, S., Ram, H., Meena, R., Singh, M., Verma, A., Kumar, U., Ghosh, A., ML, J., 2017. Strategies for improving nitrogen use efficiency: A review. *Agric. Rev.* 38 (1), 29–40.
- Yahaya, S.M., Mahmud, A.A., Abdullaht, M., Haruna, A., 2023. Recent advances in the chemistry of nitrogen, phosphorus and potassium as fertilizers in soil: a review. *Pedosphere* 33 (3), 385–406.
- Yao, Z., Yan, G., Zheng, X., Wang, R., Liu, C., Butterbach-Bahl, K., 2017. Reducing N<sub>2</sub>O and NO emissions while sustaining crop productivity in a Chinese vegetable-cereal double cropping system. *Environ. Pollut.* 231, 929–941.
- Yin, P., Chen, R., Wang, L., Meng, X., Liu, C., Niu, Y., Lin, Z., Liu, Y., Liu, J., Qi, J., You, J., Zhou, M., Kan, H., 2017. Ambient ozone pollution and daily mortality: a nationwide study in 272 Chinese cities. *Environ. Health Perspect.* 125 (11), 117006.
- Zhang, Q., Zheng, Y., Tong, D., Shao, M., Wang, S., Zhang, Y., Xu, X., Wang, J., He, H., Liu, W., Ding, Y., Lei, Y., Li, J., Wang, Z., Zhang, X., Wang, Y., Cheng, J., Liu, Y., Shi, Q., Yan, L., Geng, G., Hong, C., Li, M., Liu, F., Zheng, B., Cao, J., Ding, A., Gao, J., Fu, Q., Huo, J., Liu, B., Liu, Z., Yang, F., He, K., Hao, J., 2019. Drivers of improved PM<sub>2.5</sub> air quality in China from 2013 to 2017. *Proc. Natl. Acad. Sci.* 116 (49), 24463–24469.
- Zhu, L., Jacob, D.J., Kim, P.S., Fisher, J.A., Yu, K., Travis, K.R., Mickley, L.J., Yantosca, R.M., Sulprizio, M.P., De Smedt, I., González Abad, G., Chance, K., Li, C., Ferrare, R., Fried, A., Hair, J.W., Hanisco, T.F., Richter, D., Jo Scarino, A., Walega, J., Weibring, P., Wolfe, G.M., 2016. Observing atmospheric formaldehyde (HCHO) from space: validation and intercomparison of six retrievals from four satellites (OMI, GOME2a, GOME2b, OMPS) with SEAC<sup>4</sup>RS aircraft observations over the Southeast US. *Atmos. Chem. Phys.* 16 (21), 13477–13490.
- Zhu, L., Sun, H., Liu, L., Zhang, K., Zhang, Y., Li, A., Bai, Z., Wang, G., Liu, X., Dong, H., Li, C., 2024. Optimizing crop yields while minimizing environmental impact through deep placement of nitrogen fertilizer. *J. Integr. Agric.* (ISSN: 2095-3119).